A Goodput Distribution Model For IEEE 802.11 Wireless Mesh Networks

Ying Qu, Bryan Ng, and Winston K.G. Seah
School of Engineering & Computer Science, Victoria University of Wellington, New Zealand
Email: {ying.qu,bryan.ng,winston.seah}@ecs.vuw.ac.nz

***Abstract*—Wireless mesh networks (WMNs) deliver network services including Internet connectivity, emergency response communications, and cellular traffic offloading. Network planning plays an increasingly important role in ensuring quality of service for such heterogeneous services. Simplicity, usability and accuracy of a model are three elements common to a successful model for network planning. Whilst research has been undertaken to model the IEEE 802.11 MAC protocol with good accuracy, these models take a packet centric view thus increasing the model complexity and restricting their usefulness in network planning. We present a novel goodput distribution model for IEEE 802.11 WMNs requiring only topology information and derived specifically to be beneficial to network planning. Analysis shows the model provides accurate estimation of goodput distributions and correctly identifies starving links in a variety of topologies.**

I. Introduction

Wireless mesh networks (WMNs) are a promising technology for next generation wireless networks and provides high performance, easy-to-deploy network connectivity service [1]. WMNs have many attractive characteristics, including low-cost deployment and maintenance [2], robustness and self-management functionality [3]. For the last decade, WMNs based on WLAN architecture have become popular in homes, schools, and airports due to the ease of installation and use.

Arguably, the deployment of WMNs is sufficiently simple that planning the placement of mesh node is not normally required. However, new services and applications are increasingly being deployed over WMNs such as smart grid and cellular traffic offloading that were not originally intended to be carried over WMNs [4]. These new uses have certain performance requirements (Quality of Service – QoS) which spawned renewed interest in network planning for WMNs.

The goal of network planning is to design a network that meets the needs and performance requirements of both the subscriber and network operator [5]–[9]. The first step of planning in WMNs is to establish an accurate and realistic goodput model that represents the critical factors influencing the network performances (such as topology etc.). A measure that takes into account these critical factors is goodput distribution which refers to the maximum achievable data rate of each link in a given WMN.

For WMNs using the IEEE 802.11 media access control (MAC) protocols, the goodput relies heavily on the efficiency of the MAC. Most existing models of IEEE 802.11 MAC protocols assume ideal carrier sensing scenarios and cannot be applied directly to non-ideal carrier sensing scenarios. While some of these models have been reworked for non-ideal carrier sensing, only a few models study goodput distribution and starvation under non-ideal settings.

Existing models for goodput distribution require detailed packet level information such as packet arrival patterns, probabilistic measures of transmission/collision and flow level details, most of which are unknown during the planning phase [10]–[13]. A goodput distribution model that is a function of node placement distances, layout and geometry is highly desirable. Such a model provides a more realistic reflection of the information available to the network planner.

The key contribution of this paper is a new model for predicting the goodput distribution of individual links and for identifying link starvation in a WMN, which has been validated through extensive simulation across different topologies. Our goodput distribution model integrates two main factors central to QoS: the effect of carrier sensing mechanism and mesh node placement (topology). These factors are deemed critical because carrier sensing mechanism controls available channel capacity for each node and topology captures the cascading effect of carrier sensing mechanism between mesh nodes. A salient feature of our model is that it can be directly integrated into Geographical Information System (GIS) tools for WMN planning.

Our model focuses on non-ideal carrier sensing condition that manifests as the so-called "border effect" which significantly degrades the QoS. Border effect refers to the severe unfairness caused by the existence of border links [14]. These border links are out of each other carrier sensing range and only have neighbouring links on one side. They experience less contention and are more likely to transmit more packets than the middle links that have neighbouring links on both sides. In this case, some links between the border links may experience goodput starvation.

The rest of this paper is organized as follows. Section II summarises the related work and motivates the need for a goodput distribution model for WMN planning. Section III introduces a simple method to calculate the goodput of individual links given a linear topology. Section IV presents the simulation results followed by the conclusion in Section V.

II. Related work

Most IEEE 802.11 MAC protocol models focus on modelling the goodput of the network under ideal carrier sensing

conditions. The classic IEEE 802.11 MAC model is derived under ideal conditions and this started from Bianchi's models [15], [16] and Cali's model [17]. Both Bianchi's and Cali's models are based on the single-hop wireless networks. The model proposed by Bianchi *et al.* computed throughput using basic and hybrid carrier sensing mechanisms with the assumption of saturated sources, finite nodes, and ideal channel condition (i.e. no hidden nodes and capture [18]).

Besides the models proposed for the ideal scenarios, several studies have contributed to better understanding of the effect of non-ideal carrier sensing mechanisms on goodput in multi-hop wireless networks [19]–[24]. Multi-hop wireless networks are much different from single-hop networks because in the carrier sensing aspect ~~because~~ not all nodes in multi-hop networks are within each other's carrier sensing range. Recent papers [25], [26] show that the hidden node problem causes a cascade effect which reduces the throughput in multi-hop networks significantly below the capacity provided by the physical layer.

Ng *et al.* [22] conducted experiments to determine whether network performance in multi-hop wireless networks is limited by hidden nodes or carrier sensing mechanisms. They observed that the efficacy of carrier sensing depends on the number of active nodes within the physical carrier sensing range and the total transmission time occupied by these active nodes. Zeng *et al.* [23] analysed the effect of the basic mechanism in multi-hop scenarios and showed that it is sufficient to tune the (i) contention window size, and (ii) physical carrier sensing range of the device to achieve maximum throughput. However, these models oversimplify network topology and thus cannot identify anomalies such as starvation.

In terms of identifying starvation, some researchers have studied the border effect and unfairness in wireless networks. Mathilde *et al.* revealed that the unfairness in IEEE 802.11 wireless networks is caused by the border effect [14]. They investigated the behaviours of wireless links in small and large one-dimensional and two-dimensional networks, and provided a general characterisation of fairness but didn't address goodput distribution.

A few researchers have developed model to study both starvation and goodput distribution based on the network topology [10]–[13]. Garetto *et al.* [10] extended Bianchi's model to calculate the per-flow throughput under the assumption that the flow level statistics of all nodes in the network is ~~are~~ known. However, it is not realistic to provide detailed flow level information of all nodes and it is difficult to use this model in the planning stage because only topology and configuration parameters are known at the network planning stage.

Other models using an approach similar to Garetto's have since appeared in the literature [13], [27], [28]. The common denominator among these models is the introduction of additional state variables to track the state of the channel. Since these state variables are dependent of its neighbouring links' states, iterative computation must be used to calculate the throughput distribution. Even though these models provide a good estimate of link throughput, the computation complexity is very high even for small networks due to iterative computations and to date none of the mentioned models have documented use in network planning.

III. Analytical Goodput Model

In this section, we analyse the behaviour of IEEE 802.11 WMNs and then derive our goodput distribution model and show its usage with an example. The goodput distribution model is premised on several assumptions (listed next) for analytical tractability.

A. Assumptions

Generally, the goodput of a link in IEEE 802.11 WMNs depends on several factors spanning the physical layer and the MAC layer. We make four assumptions to simplify the analysis as follows.

(i) Nodes are configured with identical parameters and saturated traffic is assumed.
(ii) A single-channel single-radio WMN for all nodes.
(iii) The distance between two border links always exceed the carrier sensing range.
(iv) Capture effect and packet losses caused by collision are ignored.

B. Analysis of WMN behaviour

To analyse the behaviour of IEEE 802.11 WMNs, we define several variables to facilitate the discussion. The symbols for these variables together appear with a brief explanation in Table. I.

TABLE I
NOTATION: SYMBOLS AND THEIR MEANING.

Symbol	Explanation
E	Complete set of links in a WMN
R_{cs}	Carrier sensing range
p_b	The probability that the channel is busy sensed by a link
p_{id}	The probability that the channel is idle sensed by a link
p_t	The probability that a link is transmitting packets
$\bar{IS}(i)$	The independent set: the links out of R_{cs} of a given link i
$\bar{\gamma}(i)$	The conflict set: the links within R_{cs} of a given link i
$d_{l,i}$	The distance between a link l and a link i
$\chi(i)$	The number of links in the $\bar{IS}(i)$
$d_{L,B}$	The distance between a link and the left border link
$d_{R,B}$	The distance between a link and the right border link
d	The inter-link distance interval
D	The distance between two border links
$G_O(i)$	The optimistic estimate of goodput for a link i
$G_P(i)$	The pessimistic estimate of goodput for a link i

Definition 1. ***Independent set:*** *Let E denote the complete set of links in a WMN. For a tagged link i in E, the independent set,*

$$\bar{IS}(i) = \{l \in E \setminus \{i\} \mid d_{l,i} > R_{cs}\}. \quad (1)$$

whereby $d_{l,i}$ is the distance between link l and link i, R_{cs} is the carrier sensing range.

Definition 2. ***Conflict set:*** *The conflict set of a tagged link i,*

$$\bar{\gamma}(i) = \{l \in E \setminus \{i\} \mid d_{l,i} \leq R_{cs}\}. \quad (2)$$

whereby $d_{l,i}$ is the distance the distance between link l and link i, R_{cs} is the carrier sensing range and it is clear that $\bar{IS}(i) \cup \bar{\gamma}(i) \cup i = E$.

For a tagged link i, the channel can be sensed to be in one of three states $\{\textbf{\textit{busy}}, \textbf{\textit{idle}}, \textbf{\textit{transmission}}\}$, defined as follows:

Definition 3. ***busy:*** *when any other nodes within its carrier sensing range R_{cs} are transmitting packets,*

Definition 4. ***idle:*** *when all nodes within its R_{cs} including the tagged link are not transmitting packets,*

Definition 5. ***transmision:*** *the tagged link i is transmitting packets and no other links within its R_{cs} are transmitting.*

Three variables, p_b, p_{id}, and p_t refer to the probabilities of the channel state sensed by a tagged link. From the perspective of a link i, the relationship $p_b + p_t + p_{id} = 1$ holds during any time period. With these variables, we analyse a typical scenario with border effect in Fig. 1.

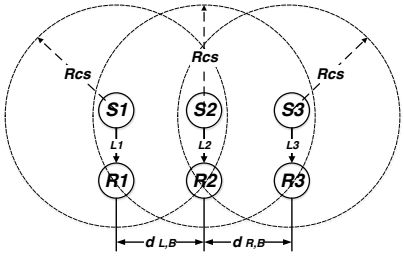

Fig. 1. The 3 links scenario.

The links $L1$ and $L3$ in Fig. 1 are the two border links that are beyond each other's R_{cs} while $L2$ is in the middle and within the R_{cs} of both $L1$ and $L3$. By the definition of $\bar{\gamma}(i)$ and $\bar{IS}(i)$, the conflict set of link of $L1$, $L2$, and $L3$ is $\{2\}, \{1,3\}, \{2\}$ while their independent set is $\{3\}, \{\emptyset\}, \{1\}$ respectively. Since the cardinality of the $\bar{\gamma}(i)$ for $L2$ is greater than $L1$ and $L3$, $L2$ will sense the channel state as busy more frequently than $L1$ and $L3$. We expect $L2$ to achieve lower goodput.

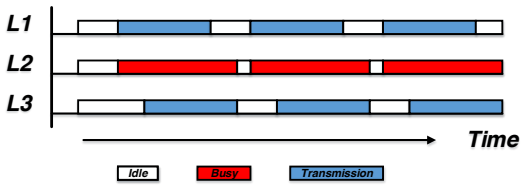

Fig. 2. Channel state with three competing links

Fig. 2 illustrates the channel state sensed by each link for the example scenario. The links $L1$ and $L3$ are independent of each other thus they cannot sense each other's transmission. Since $L2$ is dependent on $L1$ and $L3$, $L2$ can only transmit when both $L1$ and $L3$ remain in backoff for a certain period. Therefore, the probabilities p_b, p_t, and p_{id} of $L1$ and $L3$ are independent of each other and dependent of $L2$'s state, while the probabilities p_b, p_t, and p_{id} for $L2$ is dependent of the states of $L1$ and $L3$.

Compared with $L1$ and $L3$, $L2$ has more constraints because $L2$ has more conflicting links. If $L1$ and/or $L3$ continually transmit packets, $L2$ will keep waiting as it senses the channel busy for most of time. In this case, $L2$ will starve while $L1$ and $L3$ achieve high goodput.

Based on the above analysis, the probability that the channel is sensed busy p_b is proportional to the number of the links in its conflict set while the probability that a transmission occurs on a given link p_t is proportional to the number of links in its independent set. As an example, $L2$ has two conflict links and the p_b of $L2$ is greater than that of $L1$ and $L3$ that have one conflict link each. Also, the transmission probability p_t of $L1$ and $L3$ are greater than $L2$ due to the difference of independent set between them. Therefore, we postulate that goodput is proportional to the number of the links in the independent set of a given link.

In a larger network, the main reason for unfairness between border links and middle links is that the border links and the middle links sense the channel state differently due to different independent sets and conflict sets. Consequently, different cardinalities of independent sets and conflict sets yield different values of p_b and p_t. The border links have more number of links in their independent set than the links between borders and they are likely to transmit more packets. The transmission attempt of links in the middle have to contend with the border links and are more likely to back off until the channel is released by the border links. Therefore, this asymmetric back off leads to unfair sharing of channel among the links in WMNs and some middle links may starve.

C. Goodput Formulation

In this section, we develop a first order approximation for predicting goodput distribution in a WMN based on the cardinalities of independent sets $\bar{IS}(i)$ and conflict sets $\bar{\gamma}(i)$ in a scenario with border effect. We make three observations which form the hypothesis for the goodput distribution model:

(i) the border effect causes starvation if a given link is within R_{cs} of two border links,
(ii) a link will not starve if it is only within the R_{cs} of one border link,
(iii) a non-starving link shares the channel capacity proportionally with neighbouring links in its conflict set.

The sum of goodput of a given link and all conflicting links will be 1. With these observations, we derive a closed form expression for normalised goodput distribution as eqn. (3).

Definition 6. ***Goodput:*** *The goodput of a tagged link i is defined as the ratio between goodput and maximum net bandwidth.*

$$G(i) = \begin{cases} 0 & , \ d_{L,B} \leq R_{cs} \text{ and } d_{R,B} \leq R_{cs} \\ \frac{\chi(i)}{\chi(i) + \sum_{j \in \bar{\gamma}(i)} \chi(j)} & , \ \text{otherwise} \end{cases} \quad (3)$$

whereby R_{cs} is the carrier sensing range, $d_{L,B}$ is the distance between a link and the left border link, $d_{R,B}$ is the distance

between a link and the right border link, and $\chi(i)$ denotes the number of links in a given $\bar{IS}(i)$.

The first part of eqn. (3) is derived from the first observation that the border effect causes starvation, while the second part of this equation follows from the second and third observations.

The goodput in eqn. (3) can be further refined when a non-starving link shares the channel capacity with neighbouring links. This refinement arises from two distinct situations. The first situation is that the conflicting links of a given link are within each other's R_{cs}. For example, all conflicting links of $L1$ are within each other's R_{cs} in Fig. 1. In this case, the sum of goodput of a tagged link i and all conflicting links will be 1, $G(i) + \sum_{j \in \bar{\gamma(i)}} G(j) = 1$. Second situation is that the conflicting links of a given link are not all within each other's R_{cs}, for example, $L2$'s conflict set is $\{1, 3\}$ but $L1$ and $L3$ are out of each other's R_{cs}. Unlike the previous case, sum of goodput of $L2$ and its conflicting links $L1$ and $L3$ cannot exceed their total goodput1, i.e. $1 < G(i) + \sum_{j \in \bar{\gamma(i)}} G(j) \leq 2$.

To address the two distinct situations, we define the pessimistic and optimistic estimate of the goodput for a given link i. For the pessimistic estimate of goodput for a tagged link, we restrict the upper bound of the achievable goodput such that $G_P(i) + \sum_{j \in \bar{\gamma(i)}} G_P(j) = 1$. Even though the total capacity that a given link shares with its conflicting links may exceed 1, we assume that the upper bound is 1 and use eqn. (4) to calculate the goodput. We regard this goodput as the pessimistic goodput.

Definition 7. ***Pessimistic Goodput*** *$G_P(i)$: The pessimistic goodput is defined as the ratio between goodput and maximum net bandwidth, subject to $G_P(i) + \sum_{j \in \bar{\gamma(i)}} G_P(j) = 1$.*

$$G_P(i) = \frac{\chi(i)}{\chi(i) + \sum_{j \in \bar{\gamma(i)}} \chi(j)} \tag{4}$$

where $\chi(i)$ is the number of links in a given $\bar{IS}(i)$.

In terms of the optimistic estimate of the goodput, we use the conflict set of the border link for all other links in eqn. (5). It is because the border link attains the highest goodput and has the fewest number of links in its conflict set. This estimate is the optimistic goodput.

Definition 8. ***Optimistic Goodput*** *$G_O(i)$: The optimistic goodput is defined as the ratio of goodput and maximum net bandwidth, subject to $G_O(B) + \sum_{j \in \bar{\gamma(B)}} G_O(j) = 1$.*

$$G_O(i) = \frac{\chi(i)}{\chi(B) + \sum_{j \in \bar{\gamma(B)}} \chi(j)} \tag{5}$$

where $\bar{\gamma(B)}$ is the conflict set of the border link B close to the link i and $\chi(B)$ is the number of links in $\bar{IS}(B)$ and $\chi(i)$ is the number of links in a given $\bar{IS}(i)$.

D. Example: Using the model

Now, we demonstrate the utility of our model with an example in a 1000×200 m^2 topology shown in Fig. 3. It is a linear, uniformly spaced and symmetric topology. We set the network size is 1000 m and R_{cs} is 700 m. The transmitter-receiver separation of all links is 200 m. The inter-link interval d is 100 m. We calculate the independent set and conflict set of all links based on the topology information and given R_{cs} (see Table. II). The network E for this scenario is $E = \{1, 2, ..., 11\}$.

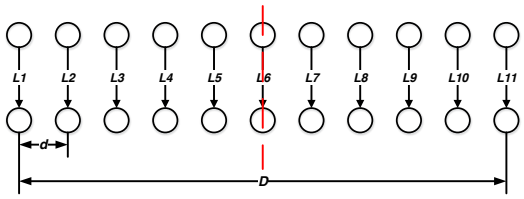

Fig. 3. 11 links in a linear, uniform and symmetric scenario

TABLE II
INDEPENDENT AND CONFLICT SETS OF INDIVIDUAL LINKS

Link i	$\bar{IS}(i)$	$\bar{\gamma}(i)$
1	$\{9, 10, 11\}$	$\{2, 3, 4, 5, 6, 7, 8\}$
2	$\{10, 11\}$	$\{1, 3, 4, 5, 6, 7, 8, 9\}$
3	$\{11\}$	$\{1, 2, 4, 5, 6, 7, 8, 9, 10\}$
4	$\{\emptyset\}$	$\{1, 2, 3, 5, 6, 7, 8, 9, 10, 11\}$
5	$\{\emptyset\}$	$\{1, 2, 3, 4, 6, 7, 8, 9, 10, 11\}$
6	$\{\emptyset\}$	$\{1, 2, 3, 4, 5, 7, 8, 9, 10, 11\}$
7	$\{\emptyset\}$	$\{1, 2, 3, 4, 5, 6, 8, 9, 10, 11\}$
8	$\{\emptyset\}$	$\{1, 2, 3, 4, 5, 6, 7, 9, 10, 11\}$
9	$\{1\}$	$\{2, 3, 4, 5, 6, 7, 8, 10, 11\}$
10	$\{1, 2\}$	$\{3, 4, 5, 6, 7, 8, 9, 11\}$
11	$\{1, 2, 3\}$	$\{4, 5, 6, 7, 8, 9, 10\}$

According to the results tabulated in Table II, links 4 to 8 are within the R_{cs} of both borders and they have no independent links. We predict that link 4 to 8 will starve and the goodput is zero. For the non-starving links, we give the weight to each link based on definition of $\chi(i)$. For example, $L3$'s independent set has only one link $L11$ so we give $L3$'s weight as 1, same for $L2$ with weight 2, and $L1$ with weight 3. Using eqn. (4) and eqn. (5), we calculate the pessimistic and optimistic goodput for this example in Table III.

TABLE III
GOODPUT ESTIMATION OF INDIVIDUAL LINKS

Link i	$\bar{IS}(i)$	$\chi(i)$	$G_P(i)$	$G_O(i)$
1	$\{9, 10, 11\}$	3	0.475	0.5
2	$\{10, 11\}$	2	0.29	0.33
3	$\{11\}$	1	0.11	0.17
4	$\{\emptyset\}$	0	0	0
5	$\{\emptyset\}$	0	0	0
6	$\{\emptyset\}$	0	0	0
7	$\{\emptyset\}$	0	0	0
8	$\{\emptyset\}$	0	0	0
9	$\{1\}$	1	0.11	0.17
10	$\{1, 2\}$	2	0.29	0.33
11	$\{1, 2, 3\}$	3	0.475	0.5

IV. VALIDATION THROUGH SIMULATION

In this section, we validate our goodput distribution model through simulations in Qualnet 5.2. We design the simulation

TABLE IV
SIMULATION CONFIGURATION PARAMETERS

Parameter Name	Value
Transmission Power	15 dBm
Receiver Sensitivity	-94 dBm
Path Loss Model	Two-Ray
Shadowing & Fading	None
Routing	Static Routing
MAC	CSMA/CA
Physical Layer	IEEE 802.11 b
Data Rate	2 Mbps
Packet Size	1500 Bytes
Interpacket Interval	10 ms

based on the assumptions in Section III: (i) we configure all nodes with identical parameters and choose constant bit rate (CBR) as the application with saturated traffic (see Table IV); (ii) all nodes are configured with one radio interface and the same channel. Mesh node placement is based on a linear uniform and symmetric topology (see Fig. 3); (iii) we choose transmitter-receiver separation as 200 m to guarantee collision-free transmissions (based on the findings from [29]) whereby it was found that carrier sensing mechanism can protect packet transmission against collision when the transmitter-receiver separation is less than $0.56 \times D_{tr}^{\max}$ ($D_{tr}^{\max}$ denotes maximum transmission range).

The theoretical $D_{tr}^{\max}$ in this simulation is approximately 427 m. This value is calculated by QualNet's radio range utility with the simulation scenario as input. Moreover, in this paper, physical carrier sensing range R_{cs} is defined by a triplet consisting of (i) the minimum receiver sensitivity of -94 dBm, (ii) maximum transmission power of 15 dBm (based on Alcatel Lucent WaveLAN card), and (iii) the two-ray propagation model, which yields a distance of 700 m.

We validate the accuracy of the model in three typical linear topologies, viz., linear uniform symmetric topology, linear asymmetric topology, and linear non-uniform topology. We show that the mean goodput from simulations fall between the $G_O(i)$ and $G_P(i)$ from our model. If so, our goodput model provides an accurate prediction for goodput distribution. The results shown for the average goodput are calculated from 100 randomly seeded simulation runs. All averages shown are reported with confidence interval of 95% given by the range of $[0.03, 3.1]$ kbps under the assumption that the averages are normally distributed.

A. Simulation Results for Linear Uniform and Symmetric Topology

In this section, we use linear uniform and symmetric topology where the inter-link distance is constant for all links (see Fig. 3). We design simulations to validate our goodput model under two conditions: (i) constant distance between two border links D and R_{cs}, varied node density; and (ii) constant node density and R_{cs}, varied D. For the first condition, we change the uniform topology by changing d. In second condition, we scale the network size by increasing D. Under both conditions, we compare the simulation results and analytical results to evaluate the accuracy of the goodput model.

- Analytical vs. Simulation with fixed border distance D and R_{cs}, varied node density

  The simulations in this scenario choose fixed border distance (1000 m) and R_{cs} (700 m). Fig. 4 to Fig. 6 demonstrate the simulation results of normalised goodput of each individual link with three different node density 50 m, 100 m, and 200 m, respectively. In each figure, the X-axis represents the link index (refer to Fig. 3 while the Y-axis represent normalised goodput from simulations , $G_O(i)$ and $G_P(i)$. From three figures, we find that the simulation results fall between $G_O(i)$ and $G_P(i)$. These results show that our analytical model is suitable for predicting goodput distribution and identifying starvation with different node densities.

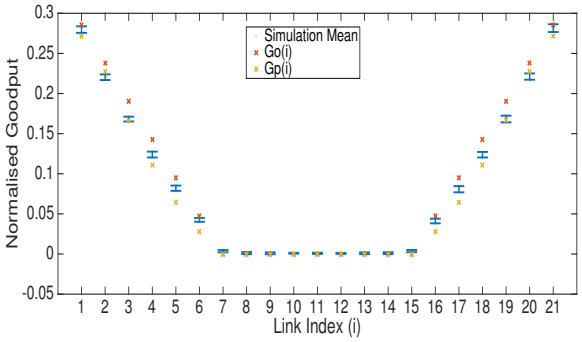

Fig. 4. Goodput of 21 links with $d = 50\,m$, $1000 \times 200\ m^2$

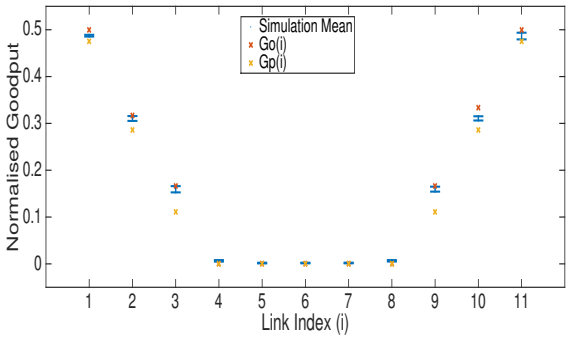

Fig. 5. Goodput of 21 links with $d = 100\,m$, $1000 \times 200\ m^2$

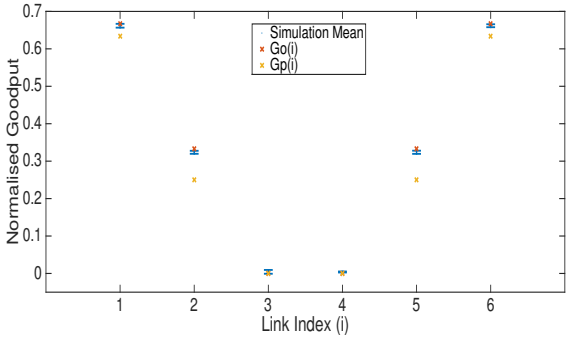

Fig. 6. Goodput of 21 links with $d = 200\,m$, $1000 \times 200\ m^2$

- Analytical vs. Simulation with fixed node density and R_{cs}, varied border distance D

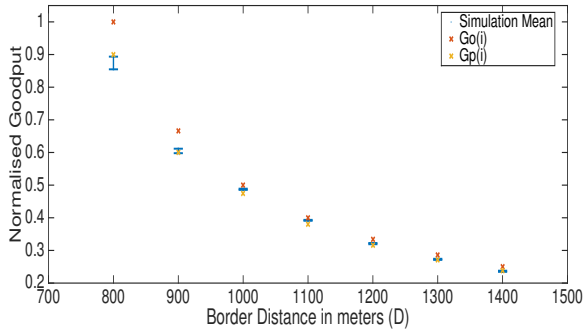

Fig. 7. Goodput of link 1 with $d = 100\,m$

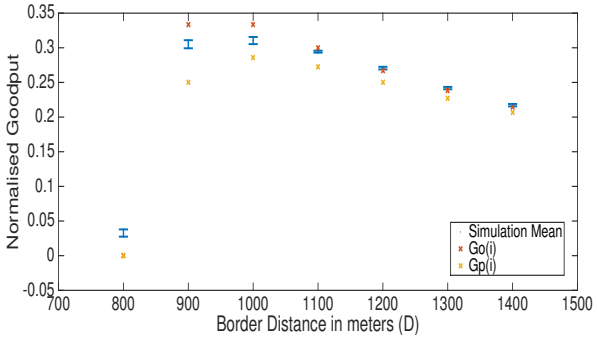

Fig. 8. Goodput of link 2 with $d = 100\,m$

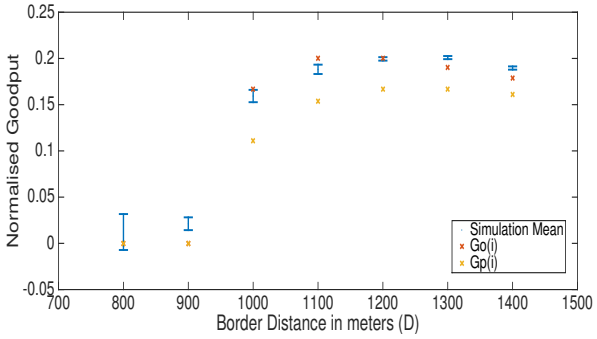

Fig. 9. Goodput of link 3 with $d = 100\,m$

In this simulation scenario, we choose fixed node density of 100 m and R_{cs} (700 m) and change D from 800 m to 1400 m. Fig. 7 to Fig. 12 illustrate the comparison between simulation results and analytical results from link 1 to link 6 (refer to Fig. 3). In each figure, the X-axis represents the border distance while the Y-axis is as same as the figures in above section. Since the topology in Fig. 3 is symmetric, we do not list the simulation results from $L7$ to $L11$ because they are as same as $L1$ to $L6$. Fig. 7 shows that the goodput of border link $L1$ resembles a negative exponential with respect to border distance D. The goodput trends of $L2$ to $L6$ are close to a typical "CSMA" curve (e.g. Chapter 4 of [30]). All simulation results are within the analytical pessimistic and optimistic

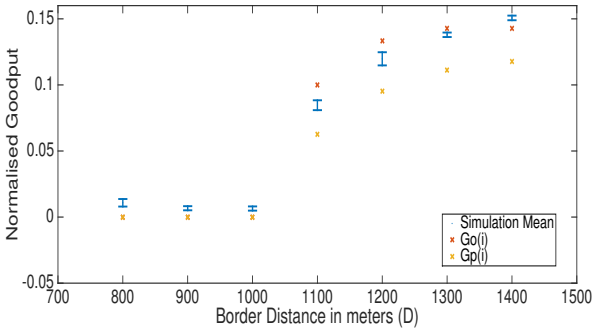

Fig. 10. Goodput of link 4 with $d = 100\,m$

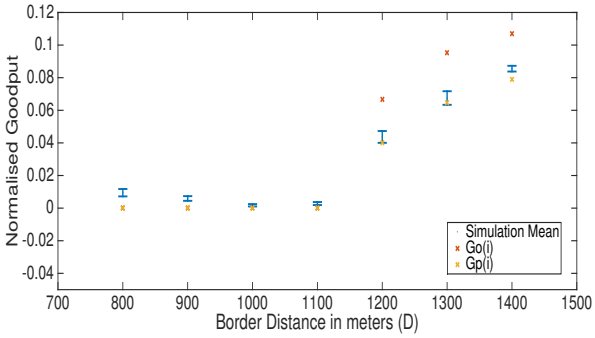

Fig. 11. Goodput of link 5 with $d = 100\,m$

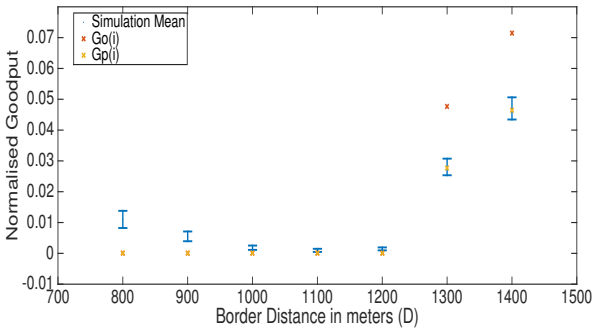

Fig. 12. Goodput of link 6 with $d = 100\,m$

values. It shows that goodput distribution is accurately predicted as a function of border distance.

B. Simulation Results For Linear Non-Uniform and Symmetric Topology

In this simulation scenario, we change the linear uniform and symmetric topology Fig. 3 to a linear non-uniform and symmetric topology by removing some links. The topology is still symmetric but d is not constant for all links. For example, we remove $L3$ and $L9$ (see Fig. 13). The results in Fig. 14 and Fig. 15 show the mean goodputs still fall between $G_O(i)$ and $G_P(i)$. It demonstrates that the analytical model is suitable for predicting goodput distribution and identifying starvation in linear non-uniform and symmetric topology.

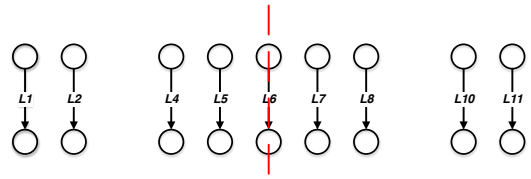

Fig. 13. 11 Links in a linear, non-Uniform and symmetric scenario

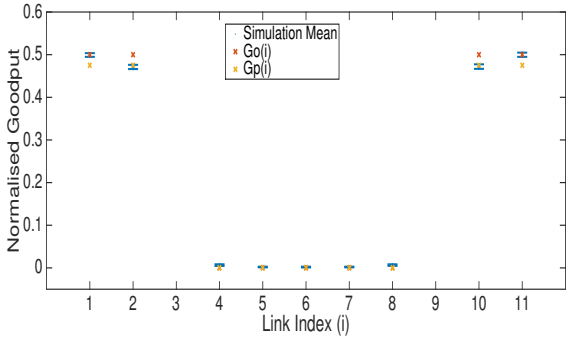

Fig. 14. Goodput distribution in non-uniform topology without links $L3$ & $L9$

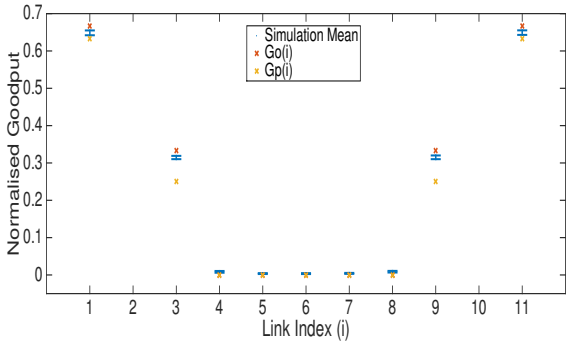

Fig. 15. Goodput distribution in non-uniform topology without links $L2$ & $L10$

C. Simulation Results For Linear Non-Uniform and Asymmetric Topology

The linear uniform and symmetric topology in Fig. 3 is modified to a linear non-uniform and asymmetric topology. The topology is asymmetric and inter-link distance is not constant. E.g., the earlier scenario in Fig. 3 results in Fig. 16 if link $L3$ is removed. The result of this scenario in Fig. 17 and Fig. 18 show our analytical model can correctly identify the starving links. However, the goodput mean value from simulation results is not always between the analytical pessimistic and optimistic expectation values. The maximum difference between simulation result and analytical result is around 4% at $i = 10$ in Fig. 17. Inaccuracy in asymmetric topology may be caused by the assumed proportional weight contributed by individual links. The reason for the inaccuracy in our analytical model is the presence of higher order dependencies is due to link asymmetry. When the topology is asymmetric, the influence of conflicting links on a tagged link may not identical and some higher order dependencies do not cancel out each other.

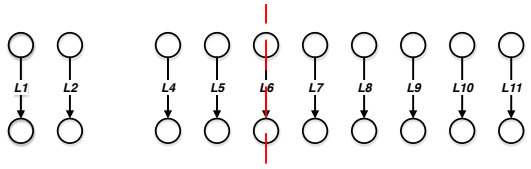

Fig. 16. 11 links in a linear, non-uniform and asymmetric scenario

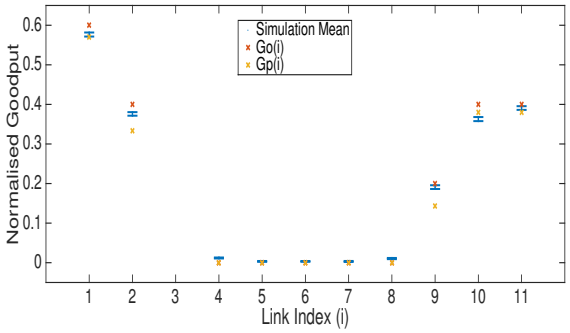

Fig. 17. Goodput distribution in non-uniform topology without link $L3$

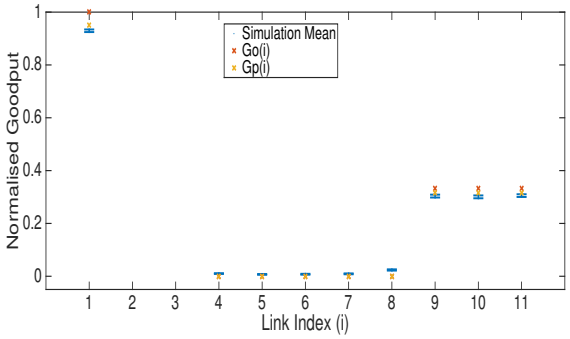

Fig. 18. Goodput distribution in non-uniform topology without links $L2$ & $L3$

D. Discussion

Based on the comparison between simulation results and analytical results, our goodput model identifies correctly the starving links and provides an accurate estimation for goodput distribution in linear topologies. In the linear non-uniform asymmetric topology, our analytical model predicts the goodput distribution with slightly higher error whereby some simulation results are out of the range of analytical predictions, $G_O(i)$ and $G_P(i)$. The model can be improved by refining weight allocation of the links in the conflict set of a tagged link.

Figure 19 shows an example of how to apply our model for network planning. The background map shows a mesh network from Kelburn campus of Victoria University of Wellington to the Te Aro campus with five access points along Ghuznee street. Given the location of these access points, our model estimates goodput distribution and identifies potential area of goodput starvation. For example, users accessing Internet through AP3 are expected to attain low goodput while users accessing the Internet through AP2 or AP1 are expected to attain higher goodput.

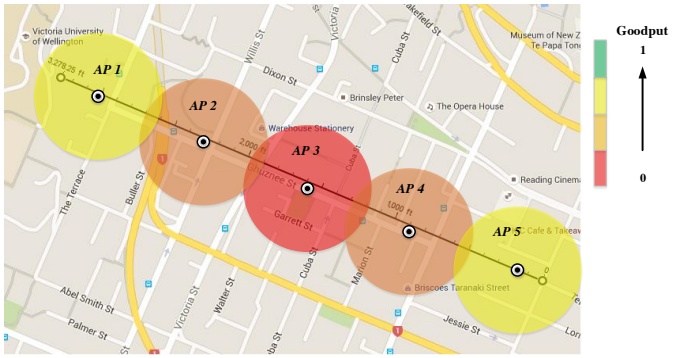

Fig. 19. Goodput distribution model used in network planning

V. CONCLUSION

In this paper, we analyse the goodput distribution of a WMN using IEEE 802.11 WLANs topology. We derive a simple goodput model based on the independent set of a tagged link. The independent set is determined by the border distance, node density, interferer proximity, and carrier sensing range. Simulations with linear topology show that our analytical model correctly identifies the starving links and provides an accurate estimate of goodput distribution with errors no more than 5%. Our model is useful for node placement and channel allocation at the network planning stage, it is being tested by the Wellington City Council through the WebMap application [31]. The results from the trials and tests will be reported elsewhere in due course.

REFERENCES

[1] I. Akyildiz and X. Wang, *Wireless mesh networks*. John Wiley & Sons, 2009, vol. 3.

[2] P. H. Pathak and R. Dutta, "A survey of network design problems and joint design approaches in wireless mesh networks," *IEEE Communications Surveys & Tutorials*, vol. 13, no. 3, pp. 396–428, 2011.

[3] E. Hossain and K. K. Leung, *Wireless mesh networks: architectures and protocols*. Springer, 2007.

[4] V. C. Güngör, D. Sahin, T. Kocak, S. Ergüt, C. Buccella, C. Cecati, and G. P. Hancke, "Smart grid technologies: communication technologies and standards," *IEEE Transactions on Industrial Informatics*, vol. 7, no. 4, pp. 529–539, 2011.

[5] A. Farsi, N. Achir, and K. Boussetta, "WLAN planning: Separate and joint optimization of both access point placement and channel assignment," *annals of telecommunications*, vol. 70, no. 5, pp. 263–274, Jun 2015.

[6] H. Zhou and C. Liu, "WLAN channel assignment based on channel overlap factor," in *Proceedings of the Second International Conference on Instrumentation, Measurement, Computer, Communication and Control (IMCCC)*, Harbin, China, 8-10 Dec 2012, pp. 249–251.

[7] A. Farsi, N. Achir, and K. Boussetta, "Three-phase heuristic algorithm for wireless LAN planning," in *Proceedings of the IEEE Wireless Communications and Networking Conference (WCNC)*, Paris, France, 1-4 April 2012, pp. 2294–2299.

[8] J. C. Rodrigues, S. C. Fraiha, J. Araújo, H. S. Gomes, C. R. L. Francês, and G. Cavalcante, "A WLAN planning proposal through direct probabilistic method and particle swarm algorithm hybrid approach," in *Proceedings of the 5th European Conference on Antennas and Propagation (EUCAP)*, Rome, Italy, 11-15 April 2011, pp. 1674–1678.

[9] J. Podolanko, S. Datta, and S. K. Das, "Performance analysis of real-time traffic over 802.11 n wireless local area networks: An experimental study," in *Proceedings of the International Wireless Communications and Mobile Computing Conference (IWCMC)*, Nicosia, Cyprus, 4-8 August 2014, pp. 453–457.

[10] M. Garetto, T. Salonidis, and E. W. Knightly, "Modeling per-flow throughput and capturing starvation in CSMA multi-hop wireless networks," *IEEE/ACM Transactions on Networking (ToN)*, vol. 16, no. 4, pp. 864–877, 2008.

[11] K. Medepalli and F. A. Tobagi, "Towards performance modeling of IEEE 802.11 based wireless networks: A unified framework and its applications," in *Proceedings of the 25th IEEE International Conference on Computer Communications (INFOCOM)*, Barcelona, Spain, 23-29 April 2006.

[12] X. Wang and K. Kar, "Throughput modelling and fairness issues in CSMA/CA based ad-hoc networks," in *Proceedings of the 24th IEEE Conference on Computer Communications (INFOCOM)*, vol. 1. IEEE, 2005, pp. 23–34.

[13] M. W. Lee, G. Hwang, and S. Roy, "Performance modeling and analysis of ieee 802.11 wireless networks with hidden nodes," in *Proceedings of the 16th ACM MSWiM*. Barcelona, Spain: ACM, 2013, pp. 135–142.

[14] M. Durvy, O. Dousse, and P. Thiran, "Border effects, fairness, and phase transition in large wireless networks," in *Proceedings of the 27th IEEE Conference on Computer Communications (INFOCOM)*, Phoenix, AZ, USA, 15-17 April 2008.

[15] G. Bianchi, "Performance analysis of the IEEE 802.11 distributed coordination function," *IEEE Journal on Selected Areas in Communications*, vol. 18, no. 3, pp. 535–547, 2000.

[16] G. Bianchi and I. Tinnirello, "Remarks on IEEE 802.11 DCF performance analysis," *IEEE Communications Letters*, vol. 9, no. 8, pp. 765–767, 2005.

[17] F. Calì, M. Conti, and E. Gregori, "Dynamic tuning of the IEEE 802.11 protocol to achieve a theoretical throughput limit," *IEEE/ACM Transactions on Networking (ToN)*, vol. 8, no. 6, pp. 785–799, 2000.

[18] K.-C. Huang and K.-C. Chen, "Interference analysis of nonpersistent CSMA with hidden terminals in multicell wireless data networks," in *Proceedings of PIMRC*, Toronto, Canada, 27-29 Sep 1995, pp. 907–911.

[19] S. H. Nguyen, H. L. Vu, and L. L. Andrew, "Performance analysis of IEEE 802.11 WLANs with saturated and unsaturated sources," *IEEE Transactions on Vehicular Technology*, vol. 61, no. 1, pp. 333–345, 2012.

[20] I. Tinnirello, G. Bianchi, and Y. Xiao, "Refinements on IEEE 802.11 distributed coordination function modeling approaches," *IEEE Transactions on Vehicular Technology*, vol. 59, no. 3, pp. 1055–1067, 2010.

[21] Y. Gao, D.-M. Chiu, and J. Lui, "Determining the end-to-end throughput capacity in multi-hop networks: methodology and applications," in *SIGMETRICS Performance Evaluation Review*, vol. 34, no. 1, 2006, pp. 39–50.

[22] P. C. Ng and S. C. Liew, "Throughput analysis of IEEE 802. 11 multi-hop ad hoc networks," *IEEE/ACM Transactions on Networking (ToN)*, vol. 15, no. 2, pp. 309–322, 2007.

[23] Z. Zeng, Y. Yang, and J. C. Hou, "How physical carrier sense affects system throughput in IEEE 802.11 wireless networks," in *Proceedings of the 27th IEEE Conference on Computer Communications (INFOCOM)*, Phoenix, AZ, USA, 15-17 Apr 2008.

[24] J. Simo Reigadas, A. Martinez-Fernandez, J. Ramos-Lopez, and J. Seoane-Pascual, "Modeling and optimizing IEEE 802.11 DCF for long-distance links," *IEEE Transactions on Mobile Computing*, vol. 9, no. 6, pp. 881–896, 2010.

[25] P. van de Ven, A. J. Janssen, and J. van Leeuwaarden, "Balancing exposed and hidden nodes in linear wireless networks," *IEEE/ACM Transactions on Networking (TON)*, vol. 22, no. 5, pp. 1429–1443, 2014.

[26] H. Zhao, E. Garcia-Palacios, S. Wang, J. Wei, and D. Ma, "Evaluating the impact of network density, hidden nodes and capture effect for throughput guarantee in multi-hop wireless networks," *Ad Hoc Networks*, vol. 11, no. 1, pp. 54–69, 2013.

[27] C. Hua and R. Zheng, "Starvation modeling and identification in dense 802.11 wireless community networks," in *Proceedings of the 27th IEEE Conference on Computer Communications (INFOCOM)*, Phoenix, AZ, USA, 15-17 April 2008.

[28] ——, "On link-level starvation in dense 802.11 wireless community networks," *Computer Networks*, vol. 54, no. 17, pp. 3159–3172, 2010.

[29] K. Xu, M. Gerla, and S. Bae, "How effective is the IEEE 802.11 RTS/CTS handshake in ad hoc networks," in *Proceedings of GLOBECOM*, Taipei, Taiwan, 17-21 Nov 2002, pp. 72–76.

[30] R. Rom and M. Sidi, *Multiple access protocols: performance and analysis*. Springer Science & Business Media, 2012.

[31] Wellington City Council, "WebMap," http://wellington.govt.nz/webmap/wccmap.html , accessed on 29 August 2015, Aug. 2015.